

# The Magnetic Behaviour of $[NnBu_4]_4[Ni_{16}Pd_{16}(CO)_{40}]$ : An Even-Electron Homoleptic Carbonyl–Metal Cluster Anion Displaying a $J=2$ Ground State

Mauro Riccò,<sup>\*[a]</sup> Toni Shiroka,<sup>[a]</sup> Stefano Carretta,<sup>[a]</sup> Fulvio Bolzoni,<sup>[b]</sup> Cristina Femoni,<sup>[c]</sup> M. Carmela Iapalucci,<sup>[c]</sup> and Giuliano Longoni<sup>\*[c]</sup>

**Abstract:** The magnetic behaviour of the even-electron  $[Ni_{16}Pd_{16}(CO)_{40}]^{4-}$  cluster, in its  $[NnBu_4]^+$  salt, has been investigated by magnetometry and muon spin rotation/relaxation ( $\mu$ SR) spectroscopy. The susceptibility measurements show an exceptionally high magnetic moment corresponding to a total spin value  $J=2$ . This suggests a Hund filling of a quadruplet ground state, quite unique in carbonyl–metal clusters. SQUID magnetometry shows a departure from the Curie–Weiss law,

for  $T > 150$  K, and strong deviation from a Brillouin behaviour of the magnetisation curves.  $\mu$ SR spectroscopy in zero applied field shows a temperature independent decay of the muon spin polarisation, similar to that of a purely paramagnetic system. The observed muon spin repolarisation in a moderate

external longitudinal field, however, invalidates this simple picture and suggests the presence of a local anisotropy field acting on the cluster's magnetic moment. A consistent interpretation of magnetometry and  $\mu$ SR results implies the occurrence of an additional interaction of the cluster spin with an effective crystalline field. The inclusion of this interaction in a model Hamiltonian allows us to successfully reproduce both the susceptibility and magnetisation data.

**Keywords:** carbonyl complexes • cluster compounds • magnetic properties • nickel • palladium

## Introduction

Only a limited number of carbonyl–metal clusters carries an odd number of valence electrons and exhibits Curie-type magnetism arising from the presence of a single unpaired electron. The overwhelming majority of carbonyl–metal clusters display an even number of electrons and are diamagnetic.<sup>[1]</sup> However, the tightening of frontier energy levels as the cluster size increases was expected to trigger magnetic behaviour in even-electron species. Consequently,

the magnetic susceptibility of several low- and high-nuclearity homometallic Ru, Os, Rh, Ni and Pt, as well as bimetallic Fe–Pt, Fe–Ag, Os–Cu, Os–Au, Os–Hg and Ni–Pt carbonyl clusters with an even number of valence electrons has been measured.<sup>[2]</sup> Some species only showed a temperature-independent paramagnetism (TIP) increasing with cluster size. Others displayed a magnetic susceptibility involving both TIP and temperature-dependent paramagnetism (TDP) contributions. The magnetic moments deduced from Curie constants were found to fall in the range 0.1–1  $\mu_B$  per cluster. In a few cases, for example,  $[Fe_3Pt_3(CO)_{15}]^{2-}$  and  $[Fe_8Ag_{13}(CO)_{32}]^{3-}$  salts, EPR experiments unambiguously demonstrated that the weak TDP was ascribed to impurities of their related odd-electron congeners, namely,  $[Fe_3Pt_3(CO)_{15}]^-$  and  $[Fe_8Ag_{13}(CO)_{32}]^{4-}$ .<sup>[3]</sup> Indeed, spin calibration experiments suggested that these odd-electron congeners were present in amounts corresponding to the measured magnetic moments.<sup>[3]</sup> Only a few clusters were found to show exceptional magnetic behaviour. Among the most notable species there were  $[Os_{40}Hg_3C_4(CO)_{96}]^{2-}$ <sup>[2e]</sup> and  $[HNi_{38}Pt_6(CO)_{48}]^{5-}$ .<sup>[2d]</sup> The former displayed a magnetic moment of 3.3  $\mu_B$  per cluster below 26 K, decreasing to 1.35  $\mu_B$  between 80 and 300 K.<sup>[2e]</sup> A theoretical qualitative framework predicting a transition from TIP (van Vleck-type), through TDP (Curie-type), to TIP (Pauli-type), as a

[a] Prof. M. Riccò, Dr. T. Shiroka, Dr. S. Carretta  
Dipartimento di Fisica and INFN, Università di Parma  
Parco Area delle Scienze 7/a, 43100 Parma (Italy)  
Fax: (+39)0521-905-223  
E-mail: mauro.riccò@fis.unipr.it

[b] Dr. F. Bolzoni  
Istituto IMEM-CNR  
Parco Area delle Scienze 37/a, 43010 Loc. Fontanini, Parma (Italy)

[c] Dr. C. Femoni, Prof. M. C. Iapalucci, Prof. G. Longoni  
Dipartimento di Chimica Fisica ed Inorganica  
Viale Risorgimento 4, 40136 Bologna (Italy)  
Fax: (+30)051-209-3711  
E-mail: longoni@ms.fci.unibo.it

function of size and metallic composition of the cluster core, was suggested.<sup>[2c]</sup>

The  $[\text{HNi}_{38}\text{Pt}_6(\text{CO})_{48}]^{5-}$  salt showed a magnetic moment of  $3.9 \mu_{\text{B}}$  per cluster as a powder sample. However, a re-determination of its magnetic moment on a single crystal<sup>[4a]</sup> failed to confirm the previous measurements and disclosed only a faint magnetism ( $0.01 \mu_{\text{B}}$  per cluster).<sup>[4b]</sup> Furthermore, DFT calculations on bare  $\text{Ni}_{44}$  and  $\text{Ni}_{38}\text{Pt}_6$ , as well as carbonylated  $[\text{Ni}_{44}(\text{CO})_{48}]^{6-}$  and  $[\text{Ni}_{38}\text{Pt}_6(\text{CO})_{48}]^{6-}$  model clusters, clearly indicated that the CO shell quenches the magnetism of the bare metal cluster.<sup>[5]</sup> These findings, as well as the extrinsic nature of TDP behaviour of  $[\text{Fe}_3\text{Pt}_3(\text{CO})_{15}]^{2-}$  and  $[\text{Fe}_8\text{Ag}_{13}(\text{CO})_{32}]^{3-}$ , cast doubts on any intrinsic TDP behaviour of carbonylated Ni and Ni–Pt clusters.

A renewed interest in magnetic behaviour of carbonyl–metal clusters was fuelled by the observation that most carbonylated Ni–Pd clusters appeared to feature extra valence electrons according to the available electron-bookkeeping rules.<sup>[6]</sup> That fact and the localised elongations of few Ni–Ni bonds in the above Ni–Pd clusters were reminiscent of the structural and electronic behaviour of the 50-electron  $[\text{Co}_3(\text{Cp})_3\text{S}_2]$  cluster.<sup>[7]</sup> To our knowledge,  $[\text{Co}_3(\text{Cp})_3\text{S}_2]$  represents the first unambiguous example of a paramagnetic organometallic cluster with an even number of electrons. A further reason of interest in the above Ni–Pd carbonylated cluster was represented by the enhanced magnetism of Ni-coated Pd and alloyed Ni–Pd nanoparticles.<sup>[8]</sup>

As a result, we have undertaken magnetic measurements of  $[\text{N}n\text{Bu}_4]_4[\text{Ni}_{16}\text{Pd}_{16}(\text{CO})_{40}]$  crystals and report here our results.

## Results and Discussion

**Structural features and EHMO calculations of  $[\text{Ni}_{16}\text{Pd}_{16}(\text{CO})_{40}]^{4-}$ :** The  $[\text{N}n\text{Bu}_4]_4[\text{Ni}_{16}\text{Pd}_{16}(\text{CO})_{40}]$  salt appeared as a suitable candidate for magnetic studies for the following reasons: 1) it is available in good yields and in a crystalline state,<sup>[6a]</sup> 2) it contains an even-electron  $[\text{Ni}_{16}\text{Pd}_{16}(\text{CO})_{40}]^{4-}$  ion, 3) related odd-electron  $[\text{Ni}_{16}\text{Pd}_{16}(\text{CO})_{40}]^{n-}$  ( $n=3$  or  $5$ ) species are unknown, 4) the anion displays a few elongated (Ni–Ni 3.01–3.12, Pd–Pd 2.95–2.99 Å) M–M contacts localised between and within the top and bottom first two layers and 5), according to electron-bookkeeping rules, it features four extra valence electrons. A view of the  $[\text{Ni}_{16}\text{Pd}_{16}(\text{CO})_{40}]^{4-}$  ion is given in Figure 1, together with

the frontier region of the molecular orbitals diagram derived from extended Hückel (EH) calculations. In agreement with electron-bookkeeping rules, EH calculations suggest the presence of a potential HOMO–LUMO gap of approximately 0.8 eV after 360 orbitals (see Figure 1, left). These MOs would formally be sufficient to lodge the valence electrons of a neutral  $[\text{Ni}_{16}\text{Pd}_{16}(\text{CO})_{40}]$  moiety. The four additional electrons present in the  $[\text{Ni}_{16}\text{Pd}_{16}(\text{CO})_{40}]^{4-}$  ion partially populate the next three tightly spaced orbitals. An analysis of the population overlap of these MO suggests their nonbonding or weakly antibonding nature with respect to the above loose M–M contacts among the metal atoms of the top and bottom first two metal layers. It seems reasonable to suggest that the four negative charges are necessary in order to stabilise the M–CO interactions and loose some M–M contacts, in synergy with some cluster swelling induced by the inner Pd atoms, which are significantly bulkier than the outer Ni atoms. Such a situation is somehow reminiscent of the  $[\text{Co}_3(\text{Cp})_3\text{S}_2]$  cluster,<sup>[7]</sup> in which the swelling effect of the face-capping sulfur atoms on the  $\text{Co}_3$  triangle and the partial population of two degenerate Co–Co antibonding orbitals coherently favour the admission of two extra valence electrons.

Although EHMO calculations can only provide a rough picture of the major features of carbonyl–metal clusters, often they are qualitatively reliable. For instance, the rough features of frontier molecular orbitals of  $[\text{Ni}_{32}\text{C}_6(\text{CO})_{36}]^{6-}$  that we can gather from EHMO and DFT calculations are largely in agreement.<sup>[4,9]</sup> Moreover, the predicted contribution of the 5s atomic orbital of the interstitial Ag atom of  $[\text{Fe}_8\text{Ag}_{13}(\text{CO})_{32}]^{4-}$  to its singly-occupied MO is closer to the experimental value for EH than for DFT calculations.<sup>[5,10]</sup> However, more subtle details such as energy and spin multiplicity cannot be safely assessed by EH. Therefore, the fact

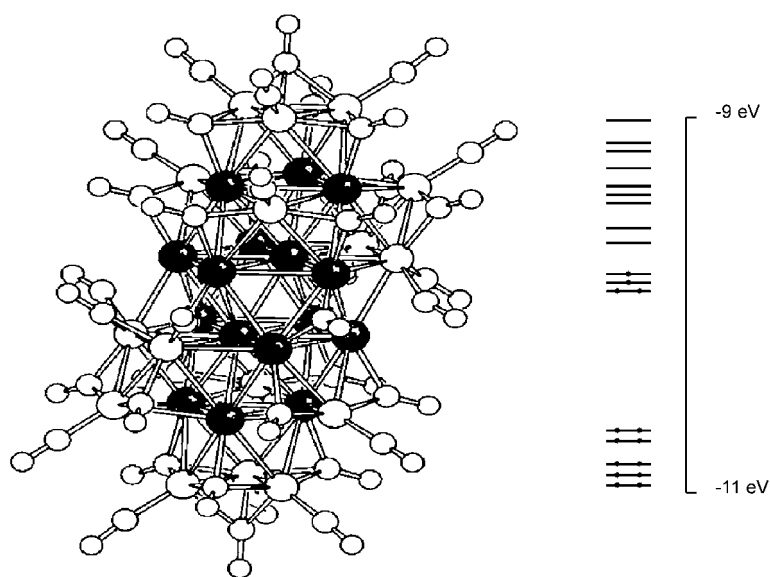


Figure 1. Left: The structure of the  $[\text{Ni}_{16}\text{Pd}_{16}(\text{CO})_{40}]^{4-}$  ion (M–M bonds  $>3 \text{ \AA}$  are omitted, Pd atoms are shown as black spheres). Right: EHMO frontier region of  $[\text{Ni}_{16}\text{Pd}_{16}(\text{CO})_{40}]^{4-}$  between  $-11$  and  $-9 \text{ eV}$ .

that the EHMO diagram of Figure 1 (left) shows two unpaired electrons cannot be taken seriously. Nevertheless, the considerations presented above aroused our curiosity to experimentally determine whether the even-electron  $[\text{Ni}_{16}\text{Pd}_{16}(\text{CO})_{40}]^{4-}$  cluster is magnetic or not.

**Magnetometry results:** The inverse molar susceptibility as a function of temperature, measured at an external field of 100 Oe, is shown in Figure 2. The reported values were mea-

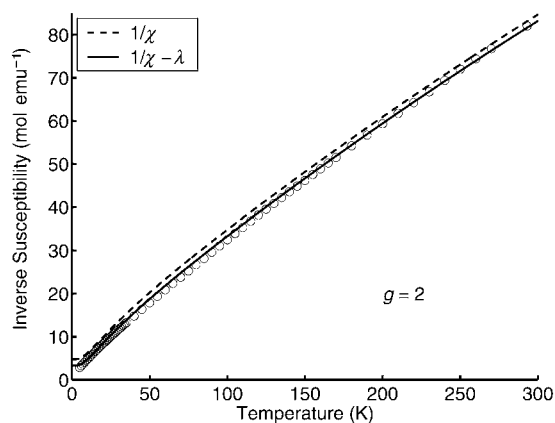


Figure 2. Inverse magnetic susceptibility versus temperature in an external field of 100 Oe suggests a paramagnetic behaviour up to 50 K. At higher temperatures, a sizeable departure from linearity is observed. A fit of the data with the model Hamiltonian [Eq. (1)] is shown: a) considering a pure paramagnetic behaviour (dashed line), and b) adding a weak ferromagnetic interaction among clusters (solid line).

sured by applying a zero-field-cooling (ZFC) procedure; no significant differences were observed in field-cooling (FC) conditions. In the temperature range 5–50 K the data follow the linear behaviour expected from a Curie–Weiss law of the type  $\chi(T-T_0)=\frac{1}{3}N(\mu_B^2 p^2/k_B)$ ; see Figure 2), in which  $N$  is the number of moles,  $\mu_B$  is the Bohr magneton and  $k_B$  is the Boltzmann constant. From the fit we find  $T_0=-3.7$  K and  $p=4.78$ , which is quite close to the value 4.9 expected for a total spin  $J=2$  (the number of effective Bohr magnetons being  $p=g\sqrt{J(J+1)}$ ), suggesting a Hund filling of a quadruplet ground state. Such a high value of the total spin is exceptional in metal–carbonyl clusters (see Introduction). The negative value of  $T_0$  could arise from a possible weak anti-ferromagnetic interaction among the magnetic moments of the clusters, although a more appropriate explanation of the experimental results will be given hereafter.

Figure 3 shows the DC magnetisation as a function of the applied field (first magnetisation curve) at two different temperatures: 5 K and 10 K; the two curves are fully reversible and no hysteresis could be estimated. The solid line represents the calculated molar magnetisation by using a Brillouin function ( $B_J$ ) with  $J=2$ . It is evident that the experimental data are not reproduced by the calculated function, which predicts a magnetisation value  $\sim 2.5$  times higher than that measured. On the other hand, if we try to fit the  $J$

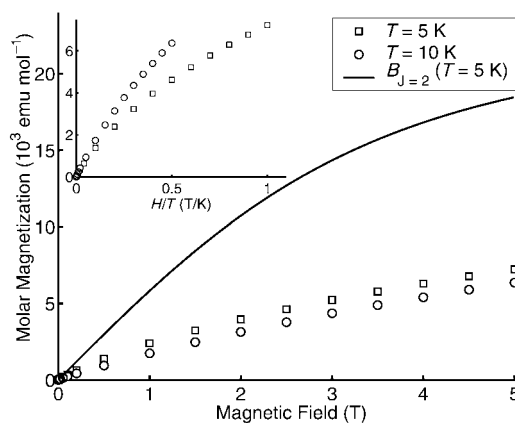


Figure 3. Molar magnetisation versus applied field at 5 and 10 K compared to the  $J=2$  Brillouin function (solid line). Inset: the renormalised data do not follow a simple Brillouin behaviour.

value with a generic  $B_J$  function, a reasonably good fit is obtained only for  $J\approx 1$ , an incompatible value with that inferred from susceptibility measurements. The deviation of magnetisation from a simple Brillouin behaviour is even more evident if the same data are plotted versus the normalised  $H/T$  value. Indeed, from the inset of Figure 3, it is clear that the two families at different temperatures do not overlap.

A consistent interpretation of the two results can be obtained by taking into account the presence of an additional interaction of the clusters' spin with an effective crystalline field, which, in our case, could arise from the elongated shape of the cluster, the bonds with the carbonyl ligands or other factors affecting the particle's magnetic moment. By assuming that at low temperatures each cluster behaves as a  $J=2$  multiplet, a quantum treatment of this effect can be performed by disregarding the details of the spin interaction and by adding only the symmetry allowed terms in the spin Hamiltonian, which, up to the second order, can be given by the following equation [Eq. (1)]:<sup>[11]</sup>

$$H_{J=2} = H_{\text{Zeeman}} + \frac{D}{3}[3J_z^2 - J(J+1)] + E(J_x^2 - J_y^2) \quad (1)$$

Further low-symmetry terms, allowed by the  $C_i$  symmetry of  $[\text{Ni}_{16}\text{Pd}_{16}(\text{CO})_{40}]^{4-}$ , have been neglected, since their inclusion did not improve the fit significantly. Since the magnetisation and susceptibility measurements were performed on powder samples, which lack of detailed information, an isotropic  $g$  factor has been assumed in the Zeeman term [Eq. (2)].

$$H_{\text{Zeeman}} = -g\mu_B B \cdot J \quad (2)$$

A least-square fit of the magnetisation data at  $T=5$  and 10 K, with the model given by Equation (1) and by using a fixed  $g=2$  factor, yields  $D=-6.7$  meV and  $|E|=2$  meV. The fit results are shown in Figure 4: the solid lines represent the calculated powder magnetisation  $M$  as a function of the applied magnetic field for  $T=5$  and 10 K. The discrep-

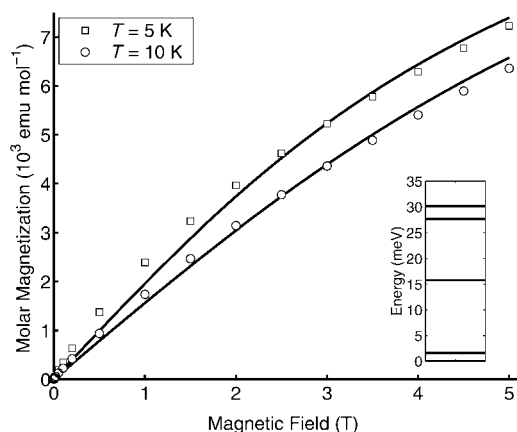


Figure 4. Fitting the magnetisation data with the model given by Equation (1) with  $D = -6.7$  meV,  $|E| = 2$  meV and  $g = 2$  (see text) gives a much better agreement.

ancy between the simulated and the experimental low-temperature and low-field data could arise because of the neglected anisotropy of the  $g$  factor or, alternatively, could be due to a nonnegligible influence of fourth-order terms in the magnetic anisotropy of each cluster. Another possible reason which would account for an underestimated  $M$  value could be the presence of small ferromagnetic interactions between neighbouring clusters. In fact, as discussed below, the discrepancy between the calculated and measured susceptibility can be recovered if a small ferromagnetic interaction is taken into account.

The zero-field level scheme calculated with the anisotropic Hamiltonian described above and the relevant best-fit parameters are shown in the inset of Figure 4. Due to the large value of the  $E/D$  ratio, the effective crystal field of  $[\text{Ni}_{16}\text{Pd}_{16}(\text{CO})_{40}]^{4+}$  splits the  $J=2$  multiplet into five well-separated singlets. The energy difference between the two lowest states is about 1.6 meV and, since the next level lies at about 15 meV higher, the 5 and 10 K magnetisation curves are determined only by the two lowest eigenstates. The least-square fitting procedure provides a second minimum for parameters  $D = 5.2$  meV and  $|E| = 1.7$  meV, which are nearly the opposite of the parameters reported above. Further measurements on single crystals will allow to unambiguously determine the Hamiltonian. In addition, it should be noted that also the sign of  $E$  in  $H_{J=2}$  cannot be established simply by measurements on powder samples, since a sign change of this parameter corresponds only to a rotation of  $90^\circ$  around the  $z$  axis.

After conjecturing the model Hamiltonian [Eq. (1)] from the magnetisation data, the second step is to check whether  $H_{J=2}$  allows us to reproduce the measured susceptibility. In presence of higher lying excited states that do not belong to the  $J=2$  manifold, the susceptibility can be written as Equation (3),<sup>[12]</sup> in which the constant  $C$  has to be determined from the experimental data.

$$\chi = \chi_{J=2} + C \quad (3)$$

By setting  $C = 2 \times 10^{-3} \text{ emu mol}^{-1}$  the dashed line in Figure 2 is obtained. Apart from a slight shift by a constant positive value  $\lambda$ , the calculated  $\chi^{-1}$  has the same shape as the experimental curve [Eq. (4)], in which  $\lambda$  is approximately  $1.5 \text{ mol emu}^{-1}$ .

$$\chi^{-1}_{\text{exp}} = \chi^{-1} - \lambda \quad (4)$$

This situation may be interpreted by considering a weak ferromagnetic interaction between neighbouring clusters, in which case  $\lambda$  would represent the molecular field constant. The calculated inverse paramagnetic susceptibility in presence of a ferromagnetic molecular field is shown in Figure 2 with a solid line. This model follows the experimental data quite well, apart perhaps at low temperatures, whereby the calculated inverse susceptibility goes to a constant value, while the measured one seems to decrease further.

The model depicted above is based on the assumption that at low temperatures each cluster behaves as an effective  $J=2$  system split by the magnetic anisotropy. It allows us to reproduce all the experimental data up to now, but more experimental and theoretical work is necessary in order to understand the origin of the observed behaviour. In addition, single-crystal experiments would allow a more precise determination of the spin Hamiltonian, especially regarding the possible tensorial nature of the coupling with the external magnetic field and the higher order anisotropy.

**Muon spin rotation/relaxation ( $\mu\text{SR}$ ) spectroscopy:** By monitoring the time evolution of implanted muon spins through the angle-resolved detection of decay positrons,  $\mu\text{SR}$  spectroscopy can provide us with useful physical information as sensed by these interstitial magnetic probes.<sup>[13a-d]</sup> To understand the nature of magnetic interactions in  $[\text{Ni}_n\text{Bu}_4]_4-[\text{Ni}_{16}\text{Pd}_{16}(\text{CO})_{40}]$  we performed both zero-field (ZF) and longitudinal-field (LF)  $\mu\text{SR}$  measurements on a powder sample, the field direction being referred to the initial muon spin polarisation.

**ZF—magnetism versus temperature:** Due to the absence of any externally applied magnetic fields, ZF represents one of the best methods to investigate intrinsic magnetic properties. The spectra at ZF were collected in the temperature range 5–300 K and each spectrum was fitted with two components: a small fast-decaying component ( $G_z(t) = G_z(0)e^{-\lambda t}$ ) and a large fixed component. The decaying signal, with an asymmetry of 6%, arises from those muons stopping near the magnetic clusters, as confirmed by LF measurements (see below). To reveal possible variations in the distribution and dynamics of the local magnetic fields with temperature, we monitored the relaxation rate of this signal.

What we found is a practically constant decay rate  $\lambda = 0.31 \pm 0.02 \mu\text{s}^{-1}$  in a relatively broad temperature range (5–60 K), compatible with a purely paramagnetic behaviour. Indeed, in the paramagnetic state, far above all magnetic freezing temperatures of a material, the electronic moments are expected to be rapidly fluctuating, and the muon spin re-

laxation function is then expected to be in the fast-fluctuation (or dynamic) limit, well described by a temperature-independent exponential decay.

At higher temperatures (60–300 K), however, a gradual decrease of  $\lambda$  takes place. This feature, which is not expected in a simple paramagnetic system, has already been observed in other magnetic molecular cluster compounds, such as  $\text{CrCu}_6$ ,  $\text{CrNi}_6$ , and  $\text{CrMn}_6$ ,<sup>[14]</sup> and indicates a decrease of the  $\omega=0$  component of the spin fluctuations spectrum at high temperatures. A detailed explanation of this behaviour is still missing, but the effect of the electron-phonon interaction within the  $J=2$  multiplet could be at the origin of the phenomenon.

**LF—repolarisation measurements:** Several longitudinal field scans in the range 0–300 mT were performed at different temperatures: 5, 30 and 75 K. The fit of the data was performed by using three components: a 13% asymmetry non-decaying background (corresponding to the muon fraction stopping in the silver frame), a field-dependent nondecaying background and a relaxing term. The amplitude of the second component as a function of the longitudinally applied field is shown in Figure 5. A maximum polarisation

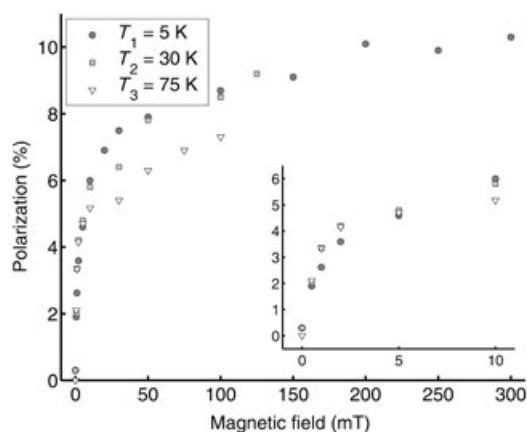


Figure 5.  $\mu\text{SR}$  repolarisation curves of  $[\text{NnBu}_4]_4[\text{Ni}_{16}\text{Pd}_{16}(\text{CO})_{40}]$  at different temperatures. The double exponential recovery (see inset) indicates the presence of two magnetically distinct species, whereas the high final saturation value does not agree with a simple paramagnetic behaviour.

value of 23%, as determined from room temperature (RT) measurements in a pure silver sample, implies that the variation range of the second component will not exceed 10%.

In general, the gradual increase of the longitudinal field determines a gradual decoupling of muon spin from the internal fields, giving a saturation of the polarisation once the decoupling is complete. When many characteristic internal fields are present one should then expect a multiexponential recovery of the muon polarisation towards its saturation value. This seems just to be the case of our LF data reported in Figure 5. Here we observe that 40% of polarisation is re-

covered within 0.4 mT (see insert), typical of muon coupling with the relatively weak nuclear magnetic moments, and most likely corresponds to the muon fraction trapped in the tetra-*n*-butylammonium counterions. This fact was confirmed also by measurements in tetra-*n*-butylammonium bromide, which presents a very similar recovery curve. On the other hand, the remaining 60% of polarisation saturates only at much higher fields, up to 200 mT. The latter recovery, typical of a static field distribution, is unexpected and does not confirm the simple paramagnetic picture deduced from the ZF measurements. It suggests that the superparamagnetic fluctuations of the cluster magnetic moment are easily dominated by the alignment action of an external magnetic field. Although unexpected in a simple paramagnet, this effect can be once more explained on the basis of a local anisotropy field which hinders the local moment fluctuation, thus confirming the interpretation of the magnetometry results given in the previous section.

## Conclusion

The magnetism of  $[\text{Ni}_{16}\text{Pd}_{16}(\text{CO})_{40}]^{4-}$  appears to be intrinsic. Beyond other considerations, an increase in magnetic moment above 150 K, as shown by susceptibility measurements, can hardly be reconciled with the presence of impurities. Therefore, the present results envision the possible existence of molecular metal–carbonyl cluster nanomagnets. The maximum spin so far observed ( $J=2$  for  $[\text{NnBu}_4]_4[\text{Ni}_{16}\text{Pd}_{16}(\text{CO})_{40}]$ ) is STILL extremely small with respect to the high-valent oxo- and cyano-bridged polynuclear compounds, which feature spin multiplicities from 3 up to 51/2.<sup>[15,16]</sup> However, it is comparable to those of other organometallic clusters. Among the latter, there are known species that undergo singlet–triplet equilibria or feature two unpaired electrons, such as the 50- or 46-electron Cp- and Cp\*-stabilised triangular clusters (e.g.,  $[\text{Co}_3(\text{Cp})_3\text{S}_2]$ ,<sup>[7]</sup>  $[\text{Co}_3(\text{Cp}^*)_3(\text{CO})_2]$ <sup>[17,18]</sup> and  $[\text{IrCo}_2(\text{Cp})_2(\text{Cp}^*)(\text{CO})_2]$ <sup>[19]</sup>). To our knowledge, the ascertained maximum spin system is 3/2 for the odd-electron  $[\text{Ni}_4(\text{Cp})_4\text{H}_3]$ <sup>[20]</sup> and  $[\text{Ni}_6(\text{Cp})_6]^+$  species,<sup>[21]</sup> and 2 for the even-electron  $[\text{Cr}_2\text{FeX}_2(\text{CO})_{10}]^{2-}$  (X = Se, Te) derivative.<sup>[22]</sup>

It may be conjectured that a progressive tightening of the frontier energy levels as a function of size of the carbonylated metal clusters could trigger magnetism in an increasing number of compounds, regardless of even or odd numbers of electrons. Novel magnetic behaviour could be at hand, since the unpaired electrons reside in molecular orbitals delocalised over most atoms of the molecule, rather than being located in atomic orbitals, as for polynuclear compounds. This difference could be at the origin of the large anisotropy suggested by the effective Hamiltonian approach. If its size is confirmed by required single-crystal measurements, this feature can envision the application of these materials as molecular magnets for information storage. Besides, it is worth recalling that the slow magnetic relaxations displayed by odd-electron  $[\text{Fe}_3\text{Pt}_3(\text{CO})_{15}]^-$ ,  $[\text{Fe}_8\text{Ag}_{13}(\text{CO})_{32}]^{4-}$  and

$[\text{Ni}_{13}\text{Sb}_2(\text{CO})_{24}]^{3-}$  species<sup>[4]</sup> are reminiscent of those of the above high-spin oxo- and cyano-bridged polynuclear compounds as well as superparamagnetic metal nanoparticles.<sup>[23]</sup>

## Experimental Section

**Materials:** The  $[\text{NnBu}_4]_4[\text{Ni}_{16}\text{Pd}_{16}(\text{CO})_{40}]$  salt was prepared according to a literature procedure<sup>[6a]</sup> by reacting  $[\text{Pd}(\text{SEt}_2)_2\text{Cl}_2]$  with  $[\text{NnBu}_4]_2[\text{Ni}_6(\text{CO})_{12}]$  in THF in a 1.6:1 molar ratio. The resulting dark brown microcrystalline precipitate was crystallised twice from acetone and *n*-hexane to obtain black prisms with a typical size in the range of 0.1–1 mm. The biggest crystals were separated and picked out with a bone microspoon and used for the measurements.

**Measurements:** DC magnetisation measurements were performed by using a Quantum Design MPMS SQUID magnetometer equipped with a home-built ultra low-field system.  $\mu\text{SR}$  measurements were performed on the EMU spectrometer at the ISIS facility (Oxford, UK). The samples, obtained by grinding ~0.5 mm average size single crystals, were manipulated in oxygen/moisture-free conditions (Ar glove box with  $\text{O}_2$  and  $\text{H}_2\text{O}$  < 1 ppm) and sealed, in both cases, in air tight cells. Special attention was devoted to temperature control to avoid thermal decomposition of the cluster (occurring above 150 °C), which would yield a sample contamination with magnetic metallic nanoparticles and, therefore, strong magnetic signals.

## Acknowledgements

We wish to acknowledge the financial support of MIUR (FIRB and PRIN 2003). We also would like to thank Prof. G. Amoretti for useful discussions and the staff of the ISIS muon facility, particularly F. Pratt, for experimental assistance.

- [1] G. Longoni, M. C. Iapalucci in *Clusters and Colloids: From Theory to Applications* (Ed.: G. Schmid), VCH, Weinheim, **1994**, p. 91; G. Longoni, C. Femoni, M. C. Iapalucci, P. Zanello, in *Metal Clusters in Chemistry, Vol II* (Eds.: P. Braunstein, L. Oro, P. Raithby), Wiley-VCH, Weinheim, **1999**, pp. 1137–1158.
- [2] a) R. E. Benfield, P. P. Edwards, A. M. Stacy, *J. Chem. Soc. Chem. Commun.* **1982**, 525; b) D. C. Johnson, R. E. Benfield, P. P. Edwards, W. H. J. Nelson, M. D. Vargas, *Nature* **1985**, *314*, 231; c) B. K. Teo, F. J. D. Salvo, J. W. Waszczak, G. Longoni, A. Ceriotti, *Inorg. Chem.* **1986**, *25*, 2262; d) B. J. Pronk, H. B. Brom, L. J. De Jongh, G. Longoni, A. Ceriotti, *Solid State Commun.* **1986**, *59*, 349; e) S. R. Drake, P. P. Edwards, B. F. G. Johnson, J. Lewis, E. A. Marsaglia, S. D. Oberstelli, N. C. Pyper, *Chem. Phys. Lett.* **1987**, *139*, 336; f) J. A. O. De Aguiar, A. Mees, J. Darriet, L. J. De Jongh, S. R. Drake, P. P. Edwards, B. F. G. Johnson, *Solid State Commun.* **1988**, *66*, 913; g) R. E. Benfield, *Z. Phys. D* **1989**, *12*, 453.
- [3] J. Sinzig, L. J. de Jongh, A. Ceriotti, R. Della Pergola, G. Longoni, M. Stener, K. Albert, N. Rosch, *Phys. Rev. Lett.* **1998**, *81*, 3211–3214; J. Sinzig, Ph.D. Thesis, University of Leiden (The Netherlands), **1998**.
- [4] a) D. A. van Leeuwen, J. M. van Ruitenbeek, L. J. de Jongh, A. Ceriotti, G. Pacchioni, O. D. Haberlen, N. Rosch, *Phys. Rev. Lett.* **1994**, *73*, 1432; b) B. J. Pronk, H. B. Brom, L. J. de Jongh, G. Longoni, A. Ceriotti, *Solid State Commun.* **1986**, *59*, 349.
- [5] N. Rösch, G. Pacchioni in *Clusters and Colloids: From Theory to Applications* (Ed.: G. Schmid), VCH, Weinheim, **1994**, p. 5, and references therein.
- [6] a) C. Femoni, M. C. Iapalucci, G. Longoni, P. H. Svensson, J. Wolowska, *Angew. Chem.* **2000**, *112*, 1702; *Angew. Chem. Int. Ed.* **2000**, *39*, 1635; b) N. T. Tran, M. Kawano, D. R. Powell, L. F. Dahl, *J. Chem. Soc. Dalton Trans.* **2000**, 4138–4144.
- [7] P. D. Frisch, L. F. Dahl, *J. Am. Chem. Soc.* **1972**, *94*, 5082–5084.
- [8] a) N. Nunomura, H. Hori, T. Teranishi, M. Miyake, S. Yamada, *Phys. Lett. A* **1998**, *249*, 524–530; b) Q. Wang, Q. Sun, J. Z. Yu, Y. Hashi, Y. Kawazoe, *Phys. Lett. A* **2000**, *267*, 394–402.
- [9] D. Collini, C. Femoni, M. C. Iapalucci, G. Longoni, P. Zanello, in *Perspect. Organomet. Chem.* **2003**, *287*, 183 and references therein.
- [10] D. Collini, C. Femoni, M. C. Iapalucci, G. Longoni, unpublished results.
- [11] M. T. Hutchings, in *Solid State Physics Vol. 16* (Eds.: F. Seitz, D. Turnbull), Academic Press, New York, **1964**, p. 227.
- [12] G. Amoretti, J. M. Fournier, *J. Magn. Magn. Mater.* **1984**, *43*, L217.
- [13] a) S. J. Blundell, *Contemp. Phys.* **1999**, *40*, 175–192; b) E. B. Karlsson, *Solid State Phenomena*, Oxford University Press, Oxford, **1995**; c) J. H. Brewer, in *Encyclopedia of Applied Physics, Vol. 11* (Ed.: G. L. Trigg), VCH, New York, **1994**, pp. 23–54; d) P. Dalmas de Rétotier, A. Yaouanc, *J. Phys. Condens. Matter* **1997**, *9*, 9113.
- [14] Z. Salman, A. Keren, P. Mendels, V. Marvaud, A. Sculler, M. Verdager, J. S. Lord, C. Baines, *Phys. Rev. B* **2002**, *65*, 132403.
- [15] D. Gatteschi, R. Sessoli, in *Magnetism: A Supramolecular Function* (Ed.: O. Kahn), Kluwer, Dordrecht, **1996**, pp. 411–430.
- [16] J. R. Long, in *Chemistry of Nanostructured Materials* (Ed.: P. Yang), World Scientific, Hong Kong, **2003**, pp. 1–25.
- [17] W. L. Olson, A. M. Stacy, L. F. Dahl, *J. Am. Chem. Soc.* **1986**, *108*, 7646–7656.
- [18] C. E. Barnes, J. A. Orvis, D. L. Staley, A. L. Rheingold, D. C. Johnson, *J. Am. Chem. Soc.* **1989**, *111*, 4992.
- [19] W. A. Herrmann, C. E. Barnes, T. Zahn, M. L. Ziegler, *Organometallics* **1985**, *4*, 172–180.
- [20] J. Muller, H. Dorner, G. Huttner, H. Lorenz, *Angew. Chem.* **1973**, *85*, 1117; *Angew. Chem. Int. Ed. Engl.* **1973**, *12*, 1005; G. Huttner, H. Lorenz, *Chem. Ber.* **1974**, *107*, 996.
- [21] M. S. Paquette, L. F. Dahl, *J. Am. Chem. Soc.* **1980**, *102*, 6621.
- [22] M. Shieh, R.-L. Chung, C.-H. Yu, M.-H. Hsu, C.-H. Ho, S.-M. Peng, Y.-H. Liu, *Inorg. Chem.* **2003**, *42*, 5477.
- [23] D. L. Leslie-Pelecky, R. D. Rieke, *Chem. Mater.* **1996**, *8*, 1770–1783.

Received: August 25, 2004

Revised: December 2, 2004

Published online: March 3, 2005